Visnyk NTUU KPI Seriia – Radiotekhnika Radioaparatobuduvannia, 2026, Iss. 103, pp. 94–102

UDC 621.314.632:621.313.2:621.3.016.25

Analysis of a Two-Stage Thyristor Rectifier Topology with Parallel Bridges for Reactive Power Reduction

Komarov V. F., Rassokhina Yu. V.

Vasyl' Stus Donetsk National University, Vinnytsia, Ukraine

E-mail: *v.komarov@donnu.edu.ua*

High-power phase-controlled thyristor DC drives, despite their reliability, have a fundamental drawback: significant reactive power consumption from the supply network, especially in dynamic operating modes with large firing angles (α). This leads to a low Displacement Power Factor (DPF) and additional losses. This study analyzes a cost-effective novel two-stage thyristor rectifier topology proposed to mitigate this problem. The topology utilizes a special transformer with secondary winding taps (e.g., at 50 % and 100 % voltage) that feed two 6-pulse bridges (R1 and R2), connected in parallel to a common DC load. The system functions as a high-speed solid-state equivalent of an On-Load Tap Changer (OLTC). By sequentially engaging the bridges, the converter maintains small firing angles (α) over a wide output voltage range. A detailed analysis of the energy characteristics, based on a case study of a typical acceleration cycle for a high-inertia drive (hoisting machine), demonstrates the topology's energy efficiency. Compared to a conventional single-bridge thyristor rectifier, the two-stage scheme reduces the total reactive energy consumed per acceleration cycle by 51 % (from 54.4 kVAr · h to 26.8 kVAr · h in the example). An additional advantage of the solution is the reduction of the Root-Mean-Square (RMS) primary winding current during the initial acceleration stage, which leads to lower active power (I^2R) losses in the transformer and supply lines. A drawback of the considered commutation algorithm is the presence of a 'discontinuous current mode' in the transformer primary winding during the mixed-mode (simultaneous operation of R1 and R2), which significantly degrades the harmonic spectrum (THD) of the input current, making the converter non-compliant with power quality standards (e.g., IEEE 519). The study concludes that practically implementing this energy-efficient topology requires hardware adaptation, specifically through the design of a custom Inter-Phase Reactor (IPR) or integration into multi-pulse configurations, to mitigate harmonic distortion while preserving the reactive power benefits.

Keywords: phase-controlled rectifier; two-stage converter; parallel-bridge rectifier; reactive power; power factor correction; high-power DC drives

DOI: 10.64915/RADAP.2026.103.94-102

Introduction

High-power DC electric drives, owing to their torque characteristics, control simplicity, reliability, and operational performance, remain the foundation of many critical industrial applications (such as rolling mills, excavators, hoisting equipment, etc.) [1].

The main driver for the modernization of such installations is the obsolescence of control platforms, which leads to a lack of spare parts and limitations in technical support.

Often, the most feasible solution is not a complete replacement of the equipment with an AC system, but rather a modernization of only the DC drive's control system. This may include replacing the entire converter or, in very high-power installations, merely updating the digital control circuitry while retaining the robust thyristor power block. This is an economically justified method of ensuring the system's continued serviceability, as demonstrated by industrial automated ecosystems with a large installed base (Siemens, ABB).

A key element of such electric drives is the thyristor converter (phase-controlled rectifier), which has gained widespread adoption due to its cost-effectiveness, high overload capability, and time-proven reliability [1,2].

However, conventional thyristor converters have an inherent drawback: the method of regulating the output voltage by changing the thyristor firing delay angle (α) is inextricably linked to the consumption of significant reactive power from the supply network [3].

Recent comprehensive reviews of thyristor rectifiers confirm that improving energy efficiency and power quality remains a primary technological challenge in modern industry [4]. Specifically, balancing the trade-offs between harmonic distortion and power factor correction is critical for high-power applications.

This problem becomes particularly acute in electric drives with high moments of inertia and prolonged dynamic operating modes, for example, with a wide speed control range or cyclic load characteristics. During acceleration stages or low-speed operation, when a low converter output voltage is required, the system is forced to operate with large firing angles. This leads to a significant phase shift between the voltage and the fundamental current harmonic, causing a sharp drop in the power factor (specifically, its component — the Displacement Power Factor, DPF).

Fluctuations in reactive power caused by heavy dynamic loads place a significant burden on the supply network, lead to increased losses in transformers and transmission lines, and can also cause power grid voltage drops, which adversely affects the operation of other equipment. Contemporary research emphasizes the need for reactive power optimization to meet the stringent voltage control requirements of modern distribution networks and clean energy production [2, 5].

Thus, the development of effective methods for reducing reactive power consumption in high-power thyristor drives remains a relevant scientific and technical challenge, aimed at improving the energy efficiency and reliability of industrial electrical systems.

A number of approaches have been proposed to solve this problem. The traditional method for improving the power quality of consumption is the use of multi-pulse rectifier circuits (12-, 18- or 24-pulse), which, by means of phase-shifting transformers [6–8] or autotransformers [9–11] as well as an Inter-Phase Reactor (IPR) [7–12], allow for the cancellation of lower-order current harmonics, effectively improving the Total Harmonic Distortion (THD).

It is also worth noting that asymmetrical firing control of series-connected bridges (sequence control) has been explored as a method to decouple active and reactive power control [13, 14]. While this technique allows for reduced reactive power consumption by operating bridges with unequal firing angles, it inherently reintroduces non-characteristic harmonics of the order $6n \pm 1$ (5th, 7th, 11th, 13th) during asymmetrical operation modes [15]. This degradation of the harmonic spectrum often negates the cancellation benefits of the 12-pulse topology, necessitating additional filtering equipment.

None of the classic multi-pulse topologies [16] fully solves the problem of reactive power consumption (DPF) without such trade-offs.

Another approach involves using mechanical On-Load Tap Changers (OLTC) on the transformer side, which allows for limiting the range of the angle α [17, 18]. However, such devices have low operating speed, are prone to mechanical wear and arcing, which also makes them unsuitable for drives with dynamic operating modes.

Modern solutions based on active power electronics, such as active power filters or rectifiers based on IGBT-transistors, are capable of achieving a near-unity power factor and sinusoidal current waveform [8, 16, 19]. At the same time, implementation of IGBT-based systems is associated with significantly higher costs, typically requiring 35...40% higher investment compared to thyristor solutions [2, 5]. Furthermore, their structural complexity [5] and the requirement for an increased number of modules can lead to potentially lower reliability [20], whereas thyristor systems are characterized by proven robustness and lower failure rates in industrial applications [2, 4, 20].

Hybrid topologies [16] are of particular interest, which combine the reliability of thyristors with controlled commutation capabilities. For example, work [21] proposed a scheme with several series-connected thyristor bridges, each of which can be short-circuited by a parallel GTO-switch. This allows for step-wise changes in the input AC voltage, maintaining a high power factor. This approach confirms the effectiveness of the stepped voltage control concept but requires the use of more complex and expensive semiconductor devices.

Recent reviews confirm that despite variable frequency drive dominance, optimizing classical topologies remains rational for high-power applications where cost and reliability are paramount [4]. However, heavy dynamic loads necessitate robust reactive power management to prevent grid instability [2], especially in modern smart distribution networks [5].

This study proposes and analyzes an alternative multi-stage thyristor rectifier topology that allows for a drastic reduction in reactive power consumption using only standard, high-reliability thyristors. The concept involves using a special transformer with taps on the secondary windings, which supply two parallel-connected thyristor bridges. Thanks to a proposed intelligent control algorithm, the system functions as a high-speed solid-state equivalent of an OLTC, ensuring a smooth transition between different voltage levels during the operation. It makes possible to maintain small thyristor firing angles over a wide output voltage range, which provides a significant improvement in power factor and substantial savings in reactive energy without the use of expensive active components.

The purpose of this article is a detailed analysis of the proposed conceptual two-stage scheme and an investigation of its energy characteristics.

1 Circuit Diagram and Principle of Operation

Let us consider the circuit diagram of the two-stage drive (Fig. 1). Here, the transformer (`Tr`) has secondary windings with additional taps providing half the output voltage.

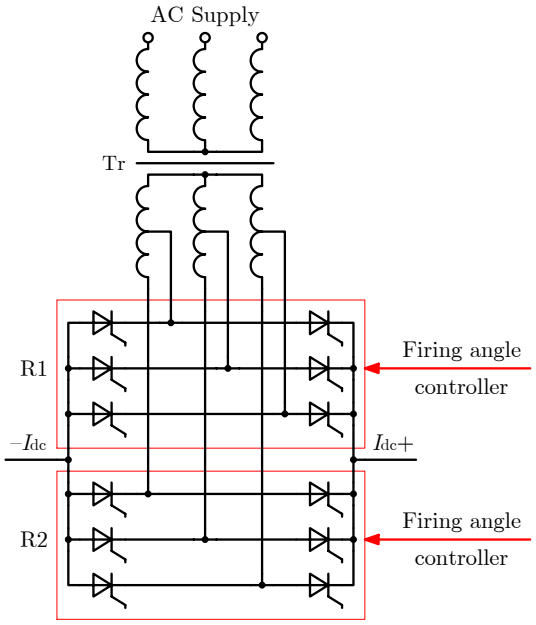

Fig. 1. Topology of the two-stage thyristor rectifier.

The windings are connected in parallel to a single load through two controlled bridge rectifiers (R1 and R2).

With this bridge connection scheme, three modes of operation are possible for the rectifier:

a) operation of bridge R1 only;

b) operation of bridge R2 only;

c) mixed mode (simultaneous operation of bridges R1 and R2).

Fig. 2 shows the timing diagrams for the operation of the proposed rectifier. Diagrams ***a***, ***b*** correspond to the operation of bridge R1, ***c*** and ***d*** — to the mixed mode, and diagrams ***e***, ***f*** — to the operation of bridge R2.

The advantage of this scheme is the ability to operate with a lower transformation ratio at a reduced voltage. Moreover, the control range of the converter's output voltage is maintained.

Let us plot the dependence of the average voltage value on the firing angles of bridges R1 and R2. When only one of the bridges is operating, we have [3]:

$$\bar{U}\left(\alpha_{\mathtt{R}}\right) = U_{\mathtt{R}} \frac{3}{\pi} \cos \alpha_{\mathtt{R}},$$

where $U_{\mathtt{R}}$ is the amplitude of the output voltage of bridge R; $\alpha_{\mathtt{R}}$ is the firing angle of bridge R.

In the case of joint operation of the bridges, the average value can be determined by integrating the values over the individual operating sections of R1 and R2 during the period T:

$$\bar{U}\left(\alpha_1, \alpha_2\right) = \\ = \frac{1}{T} \sum_n \int_{t_1^{(n)}}^{t_2^{(n)}} U_{\mathtt{R}}^{(n)} \sin\left(\omega t + \phi\left(\alpha_{\mathtt{R}}^{(n)}\right)\right) dt, \qquad (1)$$

where n is the number of the subinterval of period T with continuous operation of one of the bridges R1 or R2; $[t_1, t_2]^{(n)}$ is the n-th time interval (the division into subintervals depends on the firing angles α_1 and α_2); $U_{\mathtt{R}}^{(n)}$ is the amplitude of the output voltage in the n-th time interval.

For a three-phase circuit, the average value of the rectified voltage can be determined over $\frac{1}{6}T$ (60°). Taking into account that the joint operation of R1 and R2 corresponds to $90° \le \alpha_2 \le 30°$ at $\alpha_1 = 0°$, for a change in the firing angle of R2 within the range 60°–90°, we get

$$\bar{U} = \frac{1}{60}\left[\int_{90°}^{120°} U_{\mathtt{R1}} \cdot \sin\phi \, d\phi + \right. \\ \left. + \int_{120°}^{150°-(90°-\alpha_2)} U_{\mathtt{R1}} \cdot \sin(\phi - 60°)\, d\phi + \int_{150°-(90°-\alpha_2)}^{150°} U_{\mathtt{R2}} \cdot \sin\phi \, d\phi\right].$$

For a change in the firing angle of R2 within the range 30°–60°:

$$\bar{U} = \frac{1}{60}\left[\int_{90°}^{120°-(60°-\alpha_2)} U_{\mathtt{R1}} \cdot \sin\phi \, d\phi + \int_{120°-(60°-\alpha_2)}^{150°} U_{\mathtt{R2}} \cdot \sin\phi \, d\phi\right].$$

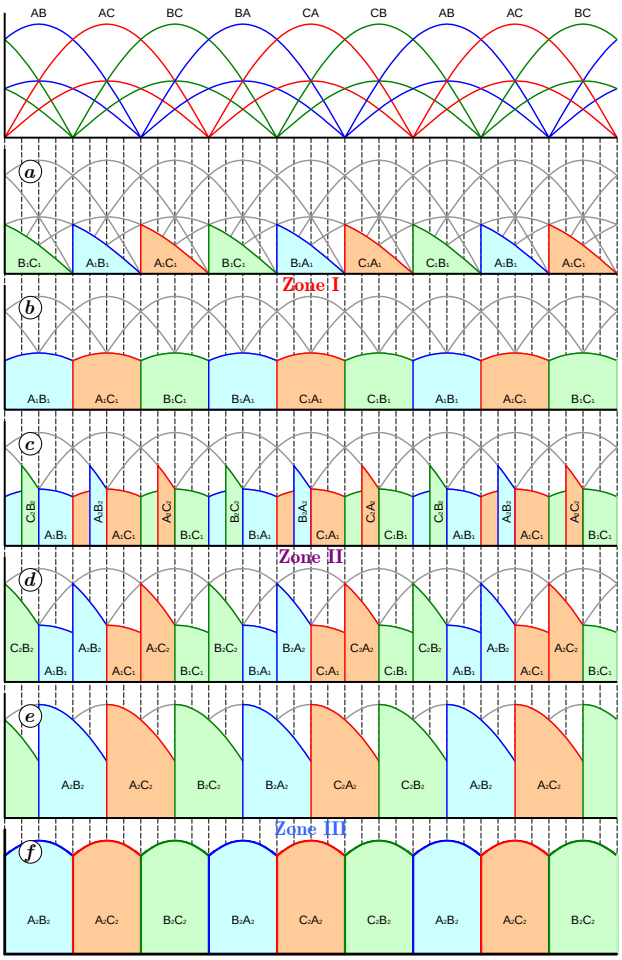

Fig. 2. Timing diagram of the two-bridge rectifier operation.

Figure 3 shows the dependence of the average voltage on the composite of firing angles during continuous commutation of bridges R1 and R2.

The continuous interval of angle values on the ordinate axis (nominal firing angle) corresponds to:

Zone I $(180° \dots 90°)$ — operation of bridge R1 with α_1 changing from 90° to 0° respectively;

Zone II $(90° \dots 30°)$ — joint operation of bridges R1 and R2 (with R1 fully open) with α_2 changing from 90° to 30° respectively;

Zone III $(30° \dots 0°)$ — operation of bridge R2 with α_2 changing from 30° to 0° respectively.

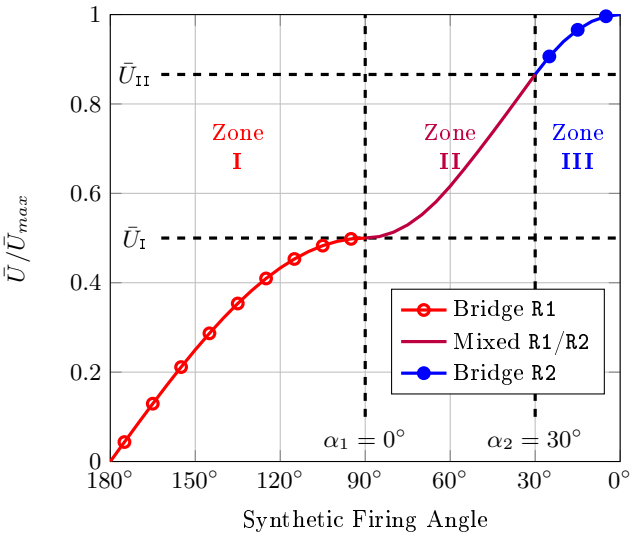

Fig. 3. Dependence of the average rectified voltage value on the firing angles of bridges R1 and R2.

To clarify the advantages of this scheme, let us analyze the consumed reactive power during the acceleration stage. To determine it, we will use the formula $Q = \sqrt{S^2 - P^2}$, where S is the apparent power; P is the active power.

Since there are three different commutation modes in this operating scheme of bridges R1 and R2, and the electric drive sequentially transitions from one mode to another during the motor acceleration process, we will divide the analysis of the acceleration period into 3 stages according to the zones in Fig. 2.

1.1 Operation of bridge R1

At the initial acceleration stage, only bridge R1 operates, which corresponds to zone I in Fig. 2.

The apparent power S_{I} consumed by the drive in this case can be calculated by the formula [3]

$$S_{\mathrm{I}} = I_{1\mathrm{L}} \cdot U_{1\mathrm{L}} \cdot \sqrt{3}.$$

where $I_{1\mathrm{L}}$ — the current of the transformer primary winding; $U_{1\mathrm{L}}$ — the network line voltage.

The current of the transformer primary winding is

$$I_{1\mathrm{L}} = K_{\mathrm{T2.1}} \cdot I_{\mathrm{dc}} \cdot \sqrt{\frac{4}{6}},$$

where $K_{\mathrm{T2.1}}$ — the transformation ratio of the winding group for bridge R1; I_{dc} — the constant motor current (a common situation is considered where acceleration occurs with constant torque on the shaft); $\sqrt{\frac{4}{6}}$ — current shape factor $\left(I_{\mathrm{RMS}} = I_{\mathrm{dc}} \cdot \sqrt{\frac{120° \times 2}{360°}}\right)$.

The active power in section I as a function of time is calculated by the formula

$$P_{\mathrm{I}}(t) \equiv P(t) = P_{\mathrm{start}} + K_{\mathrm{acc}} \cdot t, \qquad (2)$$

where $K_{\mathrm{acc}} = P_{\mathrm{nom}}/t_{\mathrm{acc}} = (U_{\mathrm{dc}} \cdot I_{\mathrm{dc}})/t_{\mathrm{acc}}$ — the rate of increase of the motor's active power during the acceleration period (t_{acc}); P_{start} — the power at the moment of start-up (depends on the nature of the drive's mechanical load and the total resistance of the motor's armature and interpole windings); P_{nom} — the nominal power (at the end of acceleration).

Then the reactive power consumed by the drive during acceleration in section I, can be calculated by the formula

$$Q_{\mathrm{I}}(t) = \sqrt{S_{\mathrm{I}}^2 - P^2(t)}.$$

1.2 Joint operation of bridges R1 and R2

After bridge R1 is fully open, bridge R2 will engage (zone II in Fig. 2).

In this case, the primary winding current will no longer be constant, and the apparent power S_{II} consumed by the drive will depend on time

$$S_{\mathrm{II}}(t) = I_{1\mathrm{L}}(t) \cdot U_{1\mathrm{L}} \cdot \sqrt{3}.$$

Let us calculate the instantaneous values of the primary winding current $I_{1\mathrm{L}}$ based on the total current law using the magnetic circuit equations.

A three-phase transformer is a branched magnetic circuit with three limbs, in each of which its own magnetic flux is enclosed. Fig. 4 corresponds to the instantaneous state during the operation of one of the bridges R1 or R2 at voltage U_{AB} (magnetic flux Φ_{AC} is not shown).

Let us write the system of equations for this case:

$$\begin{cases} 0 = I_{\mathrm{A}} W_1 - I_{\mathrm{B}} W_1 - i_a W_2 - i_b W_2 \\ 0 = I_{\mathrm{B}} W_1 - I_{\mathrm{C}} W_1 + i_b W_2 \\ 0 = I_{\mathrm{A}} + I_{\mathrm{B}} + I_{\mathrm{C}} \end{cases}, \qquad (3)$$

where I_{A}, I_{B}, I_{C} are the primary winding currents in the corresponding phases A, B, and C; i_a, i_b are the currents in the corresponding secondary windings of the transformer; W_1 and W_2 are the number of turns of the primary and secondary windings, respectively (the number of turns of the secondary winding, in this case, depends on which bridge is operating — R1 or R2).

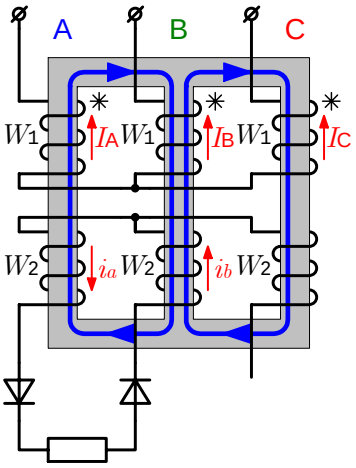

Fig. 4. For the calculation of currents in the transformer primary windings.

Let us solve the system (3) taking into account that $i_a = i_b = I_{\text{dc}}$:

$$I_A = I_{\text{dc}} \frac{W_2}{W_1} = I_{\text{dc}} K_{\text{T}},$$
$$I_B = -I_{\text{dc}} \frac{W_2}{W_1} = -I_{\text{dc}} K_{\text{T}},$$
$$I_C = 0,$$

where K_{T} — the transformation ratio of the active bridge's winding group; I_{dc} — the constant motor current during acceleration.

Knowing the control rules for bridges R1 and R2 and having solved the systems of equations for each rectifier state per one period, we can plot the timing diagram of the currents in the transformer primary windings. The diagrams in Fig. 5 correspond to $\alpha_1 = 0°$ and $\alpha_2 = 75°$.

The RMS value of the current in the primary winding in zone **II** depends on the firing angles of bridge R2 and is determined by the formula

$$I_{1\text{L}}(\alpha_2) = \sqrt{\frac{1}{T}\int_0^T f^2(\phi, \alpha_2)\, d\phi},$$

where $f(\phi)$ — the primary current function (periodic); $\alpha_2(t)$ — the firing angle of bridge R2 (in section **II**, it changes from 90° to 30°, which corresponds to a change in the average rectified voltage from $0.5\,\bar{U}_{max}$ to $0.866\,\bar{U}_{max}$).

For a change in α_2 from 90° to 60°, due to the symmetry of the half-periods in the phase A circuit, we have (4a), where K_{T1}, K_{T2} — the transformation ratios of the winding groups for bridges R1 and R2, respectively; I_{dc} — the constant motor current during acceleration. And for a change in α_2 from 60° to 30° (Fig. 6), we have (4b), respectively.

Simplification of formulas (4a) and (4b) in the section **II** from 90° to 30° yields identical results, so a general dependency can be used:

$$I_{1\text{L}}(\alpha_2) = \sqrt{\frac{1}{\pi}\left[\int_0^{\alpha_2-\frac{\pi}{3}} I_{A1}^2\, d\phi + \int_{\frac{\pi}{6}}^{\alpha_2} I_{A1}^2\, d\phi + \int_{\alpha_2}^{\frac{\pi}{2}} I_{A2}^2\, d\phi + \int_{\frac{\pi}{2}}^{\frac{2}{3}\pi} I_{A1}^2\, d\phi + \int_{\alpha_2+\frac{\pi}{3}}^{\frac{5}{6}\pi} I_{A2}^2\, d\phi\right]} = \tag{4a}$$
$$= \frac{I_{\text{dc}}}{\sqrt{\pi}} \sqrt{K_{T1}^2 \left(\int_0^{\alpha_2-\frac{\pi}{3}} d\phi + \int_{\frac{\pi}{6}}^{\alpha_2} d\phi + \int_{\frac{\pi}{2}}^{\frac{2}{3}\pi} d\phi\right) + K_{T2}^2 \left(\int_{\alpha_2}^{\frac{\pi}{2}} d\phi + \int_{\alpha_2+\frac{\pi}{3}}^{\frac{5}{6}\pi} d\phi\right)} =$$
$$= \frac{I_{\text{dc}}}{\sqrt{\pi}} \sqrt{\left(2\alpha_2 - \frac{\pi}{3}\right) K_{T1}^2 + (\pi - 2\alpha_2) K_{T2}^2},$$

$$I_{1\text{L}}(\alpha_2) = \sqrt{\frac{1}{\pi}\left[\int_{\frac{\pi}{6}}^{\alpha_2} I_{A1}^2\, d\phi + \int_{\alpha_2}^{\frac{\pi}{2}} I_{A2}^2\, d\phi + \int_{\frac{\pi}{2}}^{\alpha_2+\frac{\pi}{3}} I_{A1}^2\, d\phi + \int_{\alpha_2+\frac{\pi}{3}}^{\frac{5}{6}\pi} I_{A2}^2\, d\phi\right]} = \tag{4b}$$
$$= \frac{I_{\text{dc}}}{\sqrt{\pi}} \sqrt{K_{T1}^2 \left(\int_{\frac{\pi}{6}}^{\alpha_2} d\phi + \int_{\frac{\pi}{2}}^{\alpha_2+\frac{\pi}{3}} d\phi\right) + K_{T2}^2 \left(\int_{\alpha_2}^{\frac{\pi}{2}} d\phi + \int_{\alpha_2+\frac{\pi}{3}}^{\frac{5}{6}\pi} d\phi\right)} =$$
$$= \frac{I_{\text{dc}}}{\sqrt{\pi}} \sqrt{\left(2\alpha_2 - \frac{\pi}{3}\right) K_{T1}^2 + (\pi - 2\alpha_2) K_{T2}^2}.$$

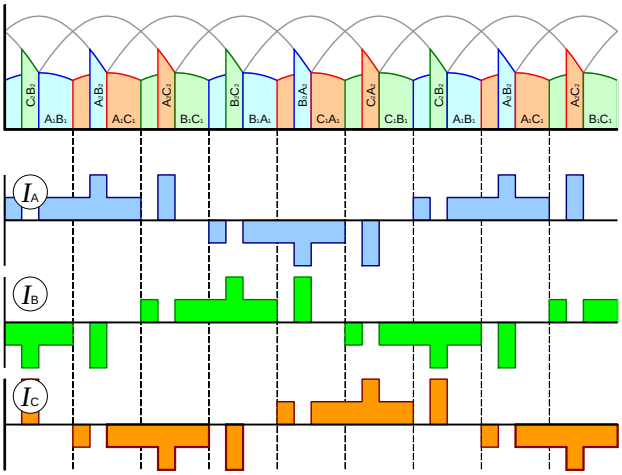

Fig. 5. Timing diagram of the phase current in the joint operation zone for $\alpha_2 = 75°$.

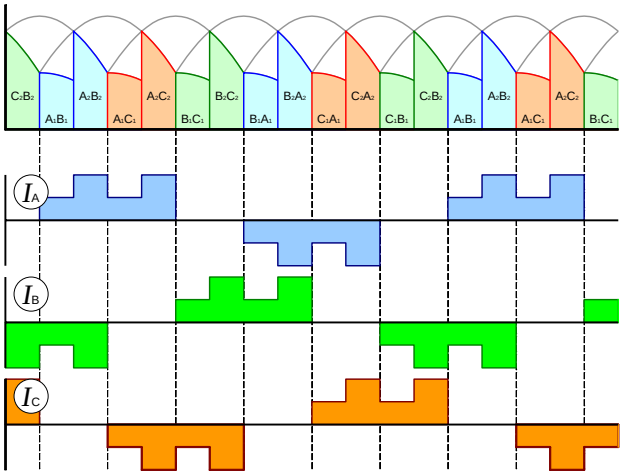

Fig. 6. Timing diagram of the phase current in the joint operation zone for $\alpha_2 = 60°$.

The dependence of the firing angle on the acceleration time is determined as the inverse function of (1), taking into account that the motor voltage during the acceleration period is $U(t) = V_r \cdot t$, where $V_r = U_M^{(end)}/t_{acc}$ is the rate of rise of the motor voltage during the acceleration period; $U_M^{(end)}$ is the motor voltage at the end of acceleration. The formula for the firing angle of bridge R2 is not provided, as numerical interpolation based on the known direct function was used in the study's calculations.

In the case of motor acceleration with constant current, the active power ($P_{II}(t)$) in section II is determined in the same way as in the case of exclusive operation of R1, by formula (2). Accordingly, the reactive power during acceleration in this section is determined by

$$Q_{II}(t) = \sqrt{S_{II}^2 - P^2(t)}.$$

1.3 Operation of bridge R2

After bridge R2 opens to 30°, the operating zone of bridge R1 is completely overlapped by bridge R2 (which corresponds to the beginning of zone III in Fig. 3).

Further motor acceleration is provided by the operation of bridge R2. The only difference for reactive power in this case (compared to the R1 case) is the larger transformation ratio of the bridge R2 windings.

The transformer primary winding current is

$$I_{1L} = K_{T2.2} \cdot I_{dc} \cdot \sqrt{\frac{4}{6}},$$

where $K_{T2.2}$ — the transformation ratio of the winding group for bridge R2 ($K_{T2.2} = 2K_{T2.1}$). As noted, motor acceleration with constant current is considered, so the active power ($P_{III}(t)$) in section III is determined by the same formula (2) as in sections I and II, and the reactive power in this section is

$$Q_{III}(t) = \sqrt{S_{III}^2 - P^2(t)}.$$

2 Analysis of Motor Acceleration with a Two-Stage Drive

As an example, let us consider the operation of an electric drive with the following parameters: supply line voltage $U_{1L} = 6000\,V$; secondary winding line voltage $U_{2L} = 712\,V$; constant motor current during acceleration $I_{dc} = 9000\,A$; motor voltage at the end of acceleration $U_{dc}^{(end)} = 740\,V$; active power during acceleration increases linearly from $P_{start} = 0.528\,MW$ to $P_{nom} = U_{dc} \cdot I_{dc} = 6.66\,MW$; acceleration period is $t_{acc} = 24\,s$; apparent power consumed by the drive (constant over the entire acceleration stage) $S = 9.06 \cdot 10^6\,VA$. The specified parameters under periodic loading are a characteristic case study for the use of a hoisting machine (mine) electric drive.

By plotting the dependencies $Q_I(t)$, $Q_{II}(t)$, and $Q_{III}(t)$, it is possible to trace the drive's reactive power consumption over the entire acceleration stage. Fig. 7 presents the corresponding graph of motor acceleration with such a two-stage electric drive.

It is evident from the graph that in the proposed scheme, with the parameters of the considered example, the motor reaches nominal speed while still in the second operating region (Zone II), and operation of bridge R2 alone (Zone III) is not used.

The difference in reactive power consumption between the converter with a conventional scheme (equivalent to the operation of bridge R2 alone) and the two-stage one (operation of R1 and joint operation of R1 and R2) is obvious.

Reactive energy consumed per acceleration cycle:

$$E_r = \int_0^{t_{acc}} Q_r(t)\,dt.$$

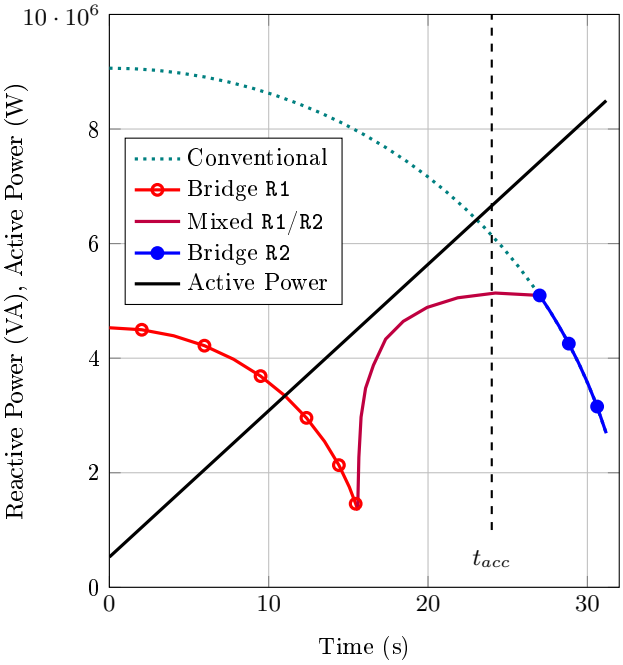

Fig. 7. Power consumption during motor acceleration with a standard and a two-stage electric drive.

In the case of a single-bridge scheme operation

$$E_{\text{r.1}} = \int_0^{t_{\text{acc}}} \sqrt{S_{\text{III}}^2 - P^2\,(t)}\,dt = 54.4\,\text{kVAr} \cdot \text{h}.$$

For the two-stage scheme (Fig. 1), it is

$$E_{\text{r.2}} = \int_0^{t_1} \sqrt{S_{\text{I}}^2 - P^2\,(t)}\,dt + \int_{t_1}^{t_{\text{acc}}} \sqrt{S_{\text{II}}^2\,(t) - P^2\,(t)}\,dt = 26.8\,\text{kVAr} \cdot \text{h}.$$

where t_1 — the moment of the drive mode change from using R1 to the joint operation of R1 and R2.

The two-stage drive allows saving approximately half ($E_{\text{r.2}}/E_{\text{r.1}} \approx 51\%$) of the excessive reactive power consumption.

Figure 8 shows the current in the transformer primary winding during the considered motor acceleration period.

As can be seen, the proposed scheme, in addition to reducing reactive power consumption, allows for energy savings by reducing active losses. The consumed current over the acceleration period is significantly lower compared to the standard single-bridge scheme.

However, with the considered switching algorithm, the proposed converter topology has one serious drawback. With the chosen bridge commutation scheme, the transformer operates with different transformation ratios during the period, and the current waveform in its primary windings is not constant for different modes. With bridge R1 fully conducting and firing angles $\alpha_2 < 60°$, the primary winding current has a discontinuous character (as shown in the timing diagram Fig. 5), which degrades its harmonic spectrum [22, 23]:

$$THD_I = \frac{\sqrt{I_5^2 + I_7^2 + I_{11}^2 + I_{13}^2}}{I_{fundamental}} \lessapprox 60\%,$$

where THD_I is the total harmonic distortion of the current waveform; $I_{fundamental}$, I_5, I_7, I_{11}, I_{13} are the fundamental, fifth, seventh, eleventh, and thirteenth (non-zero) harmonics of the primary current, respectively.

Nevertheless, a fundamental advantage of the proposed solution is its inherent compatibility with multi-pulse topologies. To ensure compliance with strict power quality standards, the system can be configured as a 12-pulse rectifier using two transformers with taps (connected in star-star and star-delta). This configuration would naturally cancel the dominant lower-order harmonics (5th and 7th), thereby partially resolving the harmonic distortion issue caused by the discontinuous current mode.

This feature distinguishes the proposed solution from asymmetrical firing control methods (sequence control) [13, 14]. While asymmetrical control also reduces reactive power, it disrupts the symmetry of operation, causing the re-emergence of non-characteristic harmonics ($6n \pm 1$) that negate the benefits of 12-pulse cancellation [15]. In contrast, the proposed tapped-transformer topology relies on amplitude regulation, preserving the phase relationships necessary for effective harmonic mitigation.

Thus, a promising direction for subsequent research is the design of a custom magnetic system (Inter-Phase Reactor and Transformers) adapted for such a two-stage, 12-pulse configuration, which would combine high energy efficiency with standard-compliant power quality.

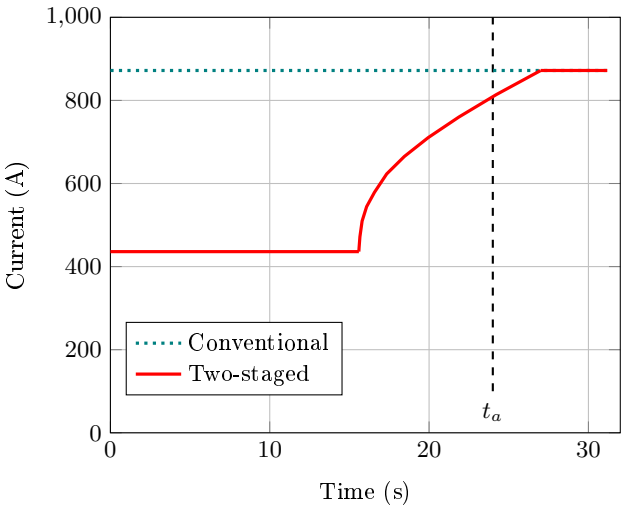

Fig. 8. Current in the transformer primary winding during acceleration (conventional vs two-stage drives).

Yet another additional way to eliminate the discontinuous current mode could be an alternative commutation option to the one considered, for example, when α_1 is fixed at 30° instead of 0°. The logic of the thyristor activation sequence in that case requires additional analysis.

Conclusions

This paper presents a conceptual two-stage thyristor rectifier topology with parallel-connected bridges, intended for high-power DC electric drives. The aim of research was the development and evaluation of a scheme capable of reducing reactive power consumption, which is a fundamental drawback of classic phase-controlled converters, especially in dynamic acceleration modes.

Case study of the proposed solution's operation under a typical acceleration cycle of high-inertial load DC motor with specified parameters, indicates the potentially high energy efficiency. Thanks to the stepped voltage control, implemented by the sequential operation of bridges connected to different transformer taps (with half and full voltage), the system is capable of maintaining a higher power factor throughout the cycle.

The proposed two-stage scheme allows for a drastic reduction in reactive energy consumption. The calculated value per acceleration cycle was 26.8 kVAr·h, which is 51% less compared to the basic single-bridge scheme (54.4 kVAr · h) under identical load conditions.

An additional advantage of the solution is the reduction of active losses (I^2R) in the transformer and supply lines, thanks to operation on the lower voltage tap (bridge `R1`) during the first acceleration stage, when the RMS value of the current in the transformer primary winding is significantly lower. This provides additional active energy savings.

A significant drawback of the considered switching algorithm with topology is the presence of a discontinuous current mode in the transformer primary winding within the joint operation zone of the bridges (Zone **II**), specifically at firing angles of bridge `R2` $\alpha_2 < 60°$. This leads to a degradation of the consumed current's harmonic spectrum and is unacceptable from the perspective of electromagnetic compatibility and power quality standards.

The proposed two-stage topology effectively addresses the reactive power minimization task, aligning with the latest trends in industrial grid optimization [5] and offering a robust alternative to complex control strategies used in similar high-power sectors [2].

Thus, although the topology demonstrates high energy efficiency, the identified problem with discontinuous currents indicates the need for further improvement. Research should be directed towards the design of a custom Inter-Phase Reactor (IPR) and the adaptation of the topology for multi-pulse configurations. This would eliminate the harmonic drawback while preserving the main energy advantages of the two-stage control.

Acknowledgements

This research was carried out within the framework of the National Research Foundation of Ukraine's program 2025.06, "Science for Strengthening the Defense Capability and National Security of Ukraine" (project No. 2025.06/0090, state registration number 0125U003181).

References

[1] Rashid, M. H. (2017). *Power Electronics Devices, Circuits And Applications*, 4th edn. Harlow: Pearson.

[2] Gao, Y., Wang, X. & Meng, X. (2024) 'Advanced rectifier technologies for electrolysis-based hydrogen production: a comparative study and real-world applications', *Energies*, 18(1), p. 48. doi: 10.3390/en18010048.

[3] Mohan, N., Undeland, T. M. & Robbins, W. P. (2002) *Power Electronics: Converters, Applications, and Design*. 3rd edn. Nashville, TN: John Wiley & Sons.

[4] Iribarren, Á., Barrios, E. L., Sanchis, P. & Ursúa, A. (2025) 'Modeling and optimal sizing of thyristor rectifiers for high-power hydrogen electrolyzers', *IEEE Journal of Emerging and Selected Topics in Power Electronics*, 13(5), pp. 5459–5478. doi: 10.1109/jestpe.2025.3566285.

[5] Zeng, Y., Qiu, Y., Xu, L., Gu, C., Zhou, Y., Li, J., Chen, S. & Zhou, B. (2025) 'Optimal investment portfolio of thyristor- and IGBT-based electrolysis rectifiers in utility-scale renewable P2H systems', *IEEE Transactions on Sustainable Energy*, pp. 1–14. doi: 10.1109/tste.2025.3595150.

[6] Oguchi, K. & Yamada, T. (1997) 'Novel 18-step diode rectifier circuit with non-isolated phase shifting transformers', *IEE Proceedings - Electric Power Applications*, 144(1), pp. 1–5. doi: 10.1049/ip-epa:19970700.

[7] Hall, J. K., Kettleborough, J. G. & Razak, A. B. M. J. (1990) 'Parallel operation of bridge rectifiers without an interbridge reactor', *IEE Proceedings B (Electric Power Applications)*, 137(2), pp. 125–140. doi: 10.1049/ip-b.1990.0013.

[8] Rodriguez, J. R. et al. (2005) 'Large current rectifiers: state of the art and future trends', *IEEE Transactions on Industrial Electronics*, 52(3), pp. 738–746. doi: 10.1109/tie.2005.843949.

[9] Gour, S. (2013) 'Comparative analysis of multipulse AC-DC converter using zigzag transformer', *IOSR Journal of Engineering*, 3(7), pp. 38–42. doi: 10.9790/3021-03753842.

[10] Voitovych, Y., Makarov, V. & Pichkalov, I. (2018) '18-pulse rectifier with electronic phase shifting with autotransformer in inverter and rectifier mode', in *2018 IEEE 6th Workshop on Advances in Information, Electronic and Electrical Engineering (AIEEE)*, Vilnius: IEEE, pp. 1–5. doi: 10.1109/aieee.2018.8592446.

[11] Singh, B. & Gairola, S. (2008) 'A zigzag connected auto-transformer based 24-pulse AC-DC converter', *Journal of Electrical Engineering & Technology*, 3(2), pp. 235–242.

[12] Choi, S., Enjeti, P. N., Lee, H.-H. & Pitel, I. J. (1996) 'A new active interphase reactor for 12-pulse rectifiers provides clean power utility interface', *IEEE Transactions on Industry Applications*, 32(6), pp. 1304–1311. doi: 10.1109/28.556632.

[13] Das, A., Chatterjee, J. K. & Gaja, A. K. (2006) 'Asymmetrical firing of 12-pulse converter for controlled P-Q operation using PIC microcontroller', in *IEEE Power India Conference*, New Delhi: IEEE, p. 5. doi: 10.1109/poweri.2006.1632602.

[14] Ahsan, F. M., Chatterjee, J. K. & Das, A. (2006) 'Operation of a 12-pulse converter in closed loop for controlled P-Q operation', in *2006 International Conference on Power Electronic, Drives and Energy Systems*, New Delhi: IEEE, pp. 1–6. doi: 10.1109/pedes.2006.344236.

[15] Hernadi, A., Taufik & Anwari, M. (2008) 'Modeling and simulation of 6-pulse and 12-pulse rectifiers under balanced and unbalanced conditions with impacts to input current harmonics', in *2008 Second Asia International Conference on Modelling & Simulation (AMS)*, Kuala Lumpur: IEEE, pp. 1034–1038. doi: 10.1109/ams.2008.88.

[16] Singh, B., Singh, B. N., Chandra, A., Al-Haddad, K., Pandey, A. & Kothari, D. P. (2004) 'A review of three-phase improved power quality AC–DC converters', *IEEE Transactions on Industrial Electronics*, 51(3), pp. 641–660. doi: 10.1109/tie.2004.825341.

[17] Zhang, M. L., Wu, B., Xiao, Y., Dewinter, F. A. & Sotudeh, R. (2002) 'A multilevel buck converter based rectifier with sinusoidal inputs and unity power factor for medium voltage (4160-7200 V) applications', *IEEE Transactions on Power Electronics*, 17(6), pp. 853–863. doi: 10.1109/TPEL.2002.805600.

[18] Kolagar, A. D. & Shoulaie, A. (2012) 'Power quality improvement in DC electric arc furnace plants utilizing multi-phase transformers', *International Transactions on Electrical Energy Systems*, 23(8), pp. 1233–1253. doi: 10.1002/ETEP.1649.

[19] Solanki, J., Fröhleke, N., Böcker, J., Averberg, A. & Wallmeier, P. (2015) High-current variable-voltage rectifiers: state of the art topologies, *IET Power Electronics*, 8(6), pp. 1068-1080. doi: 10.1049/iet-pel.2014.0533.

[20] Naseri, F. & Samet, H. (2015) 'A comparison study of high power IGBT-based and thyristor-based AC to DC converters in medium power DC arc furnace plants', in *2015 9th International Conference on Compatibility and Power Electronics (CPE)*, Lisbon: IEEE. doi: 10.1109/cpe.2015.7231042.

[21] Zargari, N. R., Xiao, Y. & Wu, B. (1997) 'A multilevel thyristor rectifier with improved power factor', *IEEE Transactions on Industry Applications*, 33(5), pp. 1208–1213. doi: 10.1109/28.633798.

[22] Blooming, T. M. & Carnovale, D. J. (2006) 'Application of IEEE STD 519-1992 Harmonic Limits', in *Conference Record of 2006 Annual Pulp and Paper Industry Technical Conference*, Appleton, WI: IEEE. doi: 10.1109/papcon.2006.1673767.

[23] IEEE (2014) *IEEE Std 519-2014: IEEE recommended practice and requirements for harmonic control in electric power systems.* New York: Institute of Electrical and Electronics Engineers.

Аналіз двоступінчастої топології тиристорного випрямляча з паралельними мостами для зменшення споживання реактивної потужності

Комаров В. Ф., Рассохіна Ю. В.

Потужні фазокеровані тиристорні електроприводи постійного струму, незважаючи на їхню надійність, мають фундаментальний недолік — значне споживання реактивної потужності з мережі живлення, особливо в динамічних режимах роботи при великих кутах керування (α). Це призводить до низького коефіцієнта зсуву (Displacement Power Factor, DPF) та додаткових втрат. Це дослідження аналізує економічно ефективну нову топологію двоступінчастого тиристорного випрямляча, запропоновану для пом'якшення цієї проблеми. Топологія використовує спеціальний трансформатор із відводами від вторинних обмоток (наприклад, на 50 % та 100 % напруги), які живлять два 6-пульсні мости (R1 та R2), підключені паралельно до спільного навантаження постійного струму. Система функціонує як швидкодіючий твердотільний аналог пристрою регулювання напруги під навантаженням. Завдяки послідовному включенню мостів у роботу перетворювач підтримує малі кути керування (α) у широкому діапазоні вихідної напруги. Детальний аналіз енергетичних характеристик на прикладному дослідженні типового циклу розгону приводу з високою інерцією (підіймальна машина) демонструє енергетичну ефективність топології. Порівняно зі звичайним одномостовим тиристорним випрямлячем, двоступінчаста схема зменшує загальну реактивну енергію, спожиту за цикл розгону, на 51 % (з 54.4 кВАр · год до 26.8 кВАр · год у прикладі). Додатковою перевагою рішення є зниження діючого (Root-Mean-Square, RMS) струму первинної обмотки на початковому етапі розгону, що призводить до зменшення активних втрат потужності (I^2R) у трансформаторі та лініях живлення. Недоліком розглянутого алгоритму комутації є наявність режиму «уривчастих» струмів у первинній обмотці трансформатора у змішаному режимі (одночасна робота R1 та R2), що значно погіршує гармонійний склад (Total Harmonic Distortion, THD) вхідного струму, роблячи перетворювач невідповідним стандартам якості електроенергії (напр., IEEE 519). У роботі зроблено висновок, що практичне впровадження цієї енергоефективної топології вимагає апаратної адаптації, зокрема проєктування спеціалізованого міжфазного реактора (Inter-Phase Reactor, IPR) або інтеграції у багатопульсні конфігурації, щоб нівелювати гармонійні спотворення, зберігаючи при цьому виграш у реактивній потужності.

Ключові слова: фазокерований випрямляч; двоступінчастий перетворювач; випрямляч з паралельними мостами; реактивна потужність; корекція коефіцієнта потужності; потужні електроприводи постійного струму